HEI Energy Collett Research Report 232

Measuring and Modeling Air Pollution and Noise Exposure Near Unconventional Oil and Gas Development in Colorado

Jeffrey L. Collett Jr. et al.

Appendix C. Supplementary Information for Chapter 4: Modeling Volatile Organic Compound Emissions and Atmospheric Dispersion of UOGD Preproduction and Early Production Activities

Correspondence may be addressed to Dr. Jeffrey L. Collett Jr., Colorado State University, Atmospheric Science Department, Fort Collins, CO 80523-1371; email: collett@atmos.colostate.edu

Although this report was produced with partial funding by the United States Environmental Protection Agency under Contract No. 68HERC19D0010 to the Health Effects Institute, it has not been subjected to the Agency's peer and administrative review and may not reflect the views of the Agency; thus, no official endorsement by the Agency should be inferred. This report also has not been reviewed by private party institutions, including those that support HEI Energy, and may not reflect the views or policies of these parties; thus, no endorsement by them should be inferred.

© 2025 Health Effects Institute, 75 Federal Street, Suite 1400, Boston, MA 02110

Appendix C. Supplementary Information for Chapter 4: Modeling Volatile Organic Compound Emissions and Atmospheric Dispersion of UOGD Preproduction and Early Production Activities

Table of Contents

C.1. Broomfield O&G Well Pads Development Timelines and Air Quality Monitoring Program

In Broomfield, Colorado, six oil and gas (O&G) well pads were developed between 2019 and 2022. The preproduction development timelines of each O&G well pad are shown in Figure C1, including drilling, hydraulic fracturing, coiled tubing/millout, production tubing installation, and flowback. After flowback, production begins. For these six O&G well pads, the preproduction developments included here spanned 192 weeks (from 2019-04-18 to 2022-12-29).

According to O&G well pad-development schedules, the AQM began in October 2018, before the start of development of the first well pad, and contained multiple monitoring sites. Details can be found in Ku et al. (2024). Some of these sites were set up near the well pads, and one was set up at a background/reference location several kilometers from the new UOGD activities. Weekly whole air canister samples collected at these sites were scheduled based on the operational timelines of nearby O&G well pads. Therefore, the sampling schedules varied from site to site. Figure C2 depicts the sampling timeline for each site in Broomfield. Samples were collected at COM, the background/reference site, continuously active throughout the whole period except for 2 weeks. Weekly samples at other monitoring sites were not always continuous because the quantity of active monitoring sites for each week varied in accordance with operations at nearby O&G well pads.

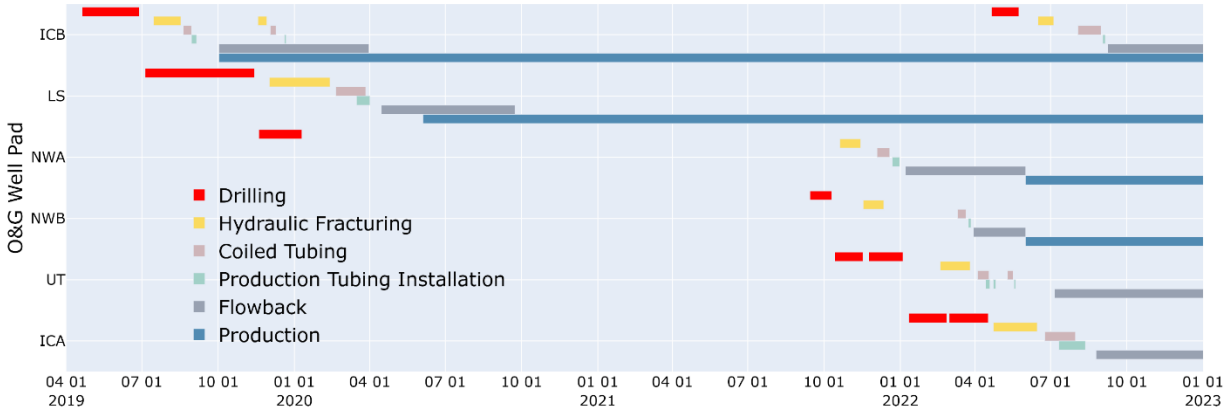

Figure C1. Development timelines of six O&G well pads in Broomfield.

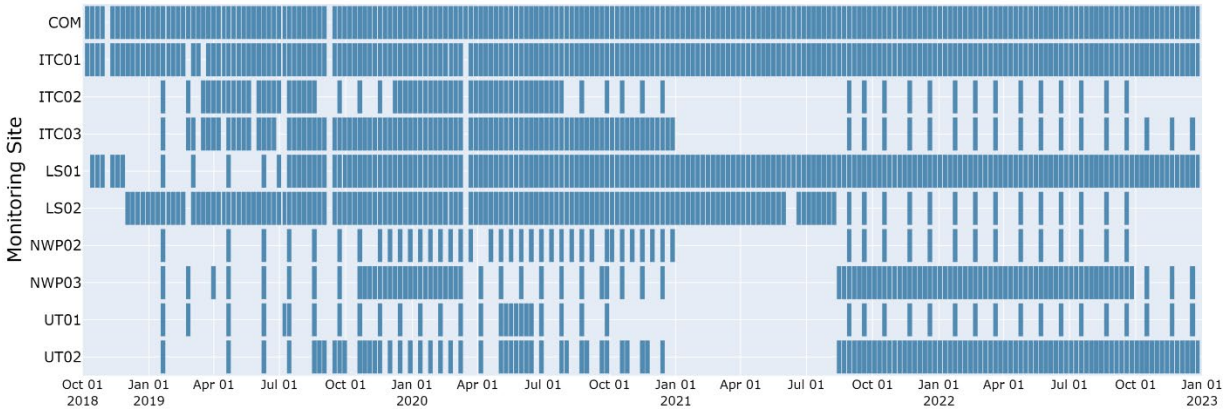

Figure C2. Weekly sampling timelines for 10 air monitoring sites in Broomfield.

C.2. Wind Data Comparison

The US Environmental Protection Agency (US EPA) recommends using meteorological data from National Weather Service stations (Perry et al. 2005). The closest station to the Broomfield area is at Denver International Airport (DIA). The DIA station provides hourly surface and twice-daily upper air meteorological data. However, the study areas are approximately 60 km away from DIA. Considering the influence of complex terrain that is much closer to Broomfield than to DIA and that the local wind field can change dramatically during a short period of time, the meteorological data from the DIA station might not be representative of our study area. As an alternative to NWS station data, the US EPA also suggests using the prognostic meteorological data generated by the Weather Research and Forecasting (WRF) model. We obtained both meteorological data sets (DIA & WRF), with the WRF data provided by Lakes Environmental Consultants Inc. We found that even with the supplementary ASOS wind data prepared by AERMINUTE, some values are still missing in the DIA data set. For example, as of September 2024, the DIA upper air sounding data after July 9, 2022, are not published. Using the WRF reanalysis data set can avoid problems with such missing values. Moreover, the airport only provides twice-daily upper air sounding data, which is extrapolated into hourly upper air data by AERMET, while the WRF data provides a higher resolution for the upper air meteorology.

In situ hourly winds collected at the meteorology site (orange dot in Figure 1, 39.9835° N, 105.0362° W) are compared with WRF and DIA wind data for the period from January to June 2022. The site is close to all the monitoring sites (<5 km). The in situ wind data were measured at a height of 5.6 meters above the ground, whereas WRF and DIA wind data were reported at 10 meters. Therefore, we adjusted the in situ wind speed (WS) to 10 meters using Equation C1 (Stull 1988), where z is the height of the wind (z_2 = 10m and z_1 = 5.6m); u is the WS at the given height; d is the displacement height; and z_0 is the surface roughness length. The log wind profile is valid for neutral conditions. We did not include the corrections for non-neutral conditions to avoid introducing additional uncertainties. Given that the measurement site is in a grassland, $d << z_1$ and z_2, and is ignored. The value of z_0 is obtained from the WRF meteorological data, taking into account the local terrain.

$$u(z_2) = u(z_1) \cdot \frac{\ln\left(\frac{z_2 - d}{z_0}\right)}{\ln\left(\frac{z_1 - d}{z_0}\right)} \quad \text{(C1)}$$

Figure C3 presents the hourly averaged wind direction (WD) and WS from WRF and DIA compared with in situ measurements, while Figure C4 shows the daily averaged wind comparison. Wind directions (left panels in Figure C3 – 4) are colored by WS. Wind speeds (right panels in Figure C3 – 4) are compared with in situ measurements using orthogonal distance regression (ODR). The comparisons include mean bias, mean error, normalized mean bias (NMB), and root mean square error (RMSE) of both WRF and DIA wind data.

Analysis of Figure C3 – 4 reveals that DIA WD observations are more consistent with in situ WD measurements than those of WRF. When low WS values (< 2 m/s) are excluded, the majority of DIA WD data points fall near the 1:1 line in relation to in situ WD, while WRF WD data show greater scattering (Figure C5 – 6). Furthermore, DIA WD observations exhibit a smaller mean bias compared to WRF, reflecting the limitations in WRF's ability to simulate WD accurately. Conversely, the ODR slope between WRF WS and in situ WS is closer to 1 than the slope between DIA WS and in situ WS. WRF WS values show lower mean bias, mean error, RSME, and NMB than DIA WS measurements, indicating that DIA wind measurements likely underestimate WS.

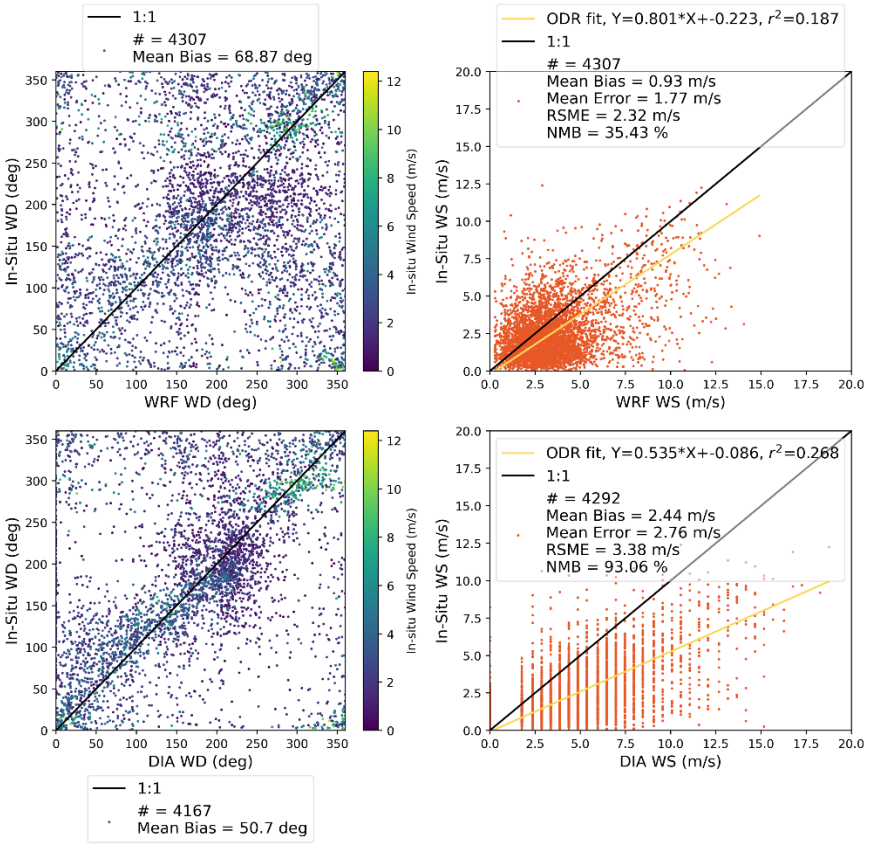

Figure C3. Hourly wind direction and wind speed comparison between in situ observations and WRF (upper panels) and DIA (lower panels) for January to June 2022. Wind directions are colored by wind speed. Mean bias, mean error, normalized mean bias (NMB), and root mean square error (RMSE) are calculated.

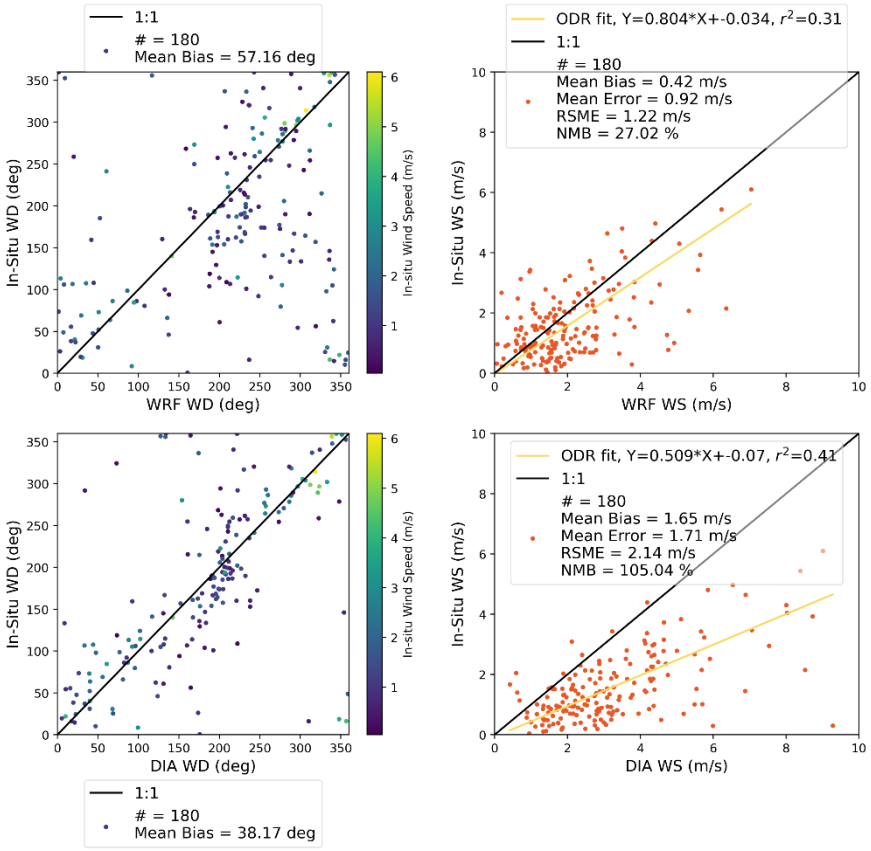

Figure C4. Daily wind direction and wind speed comparison between in situ observations and WRF (upper panels) and DIA (lower panels) for January to June 2022. Wind directions are colored by wind speed. Mean bias, mean error, normalized mean bias (NMB), and root mean square error (RMSE) are calculated.

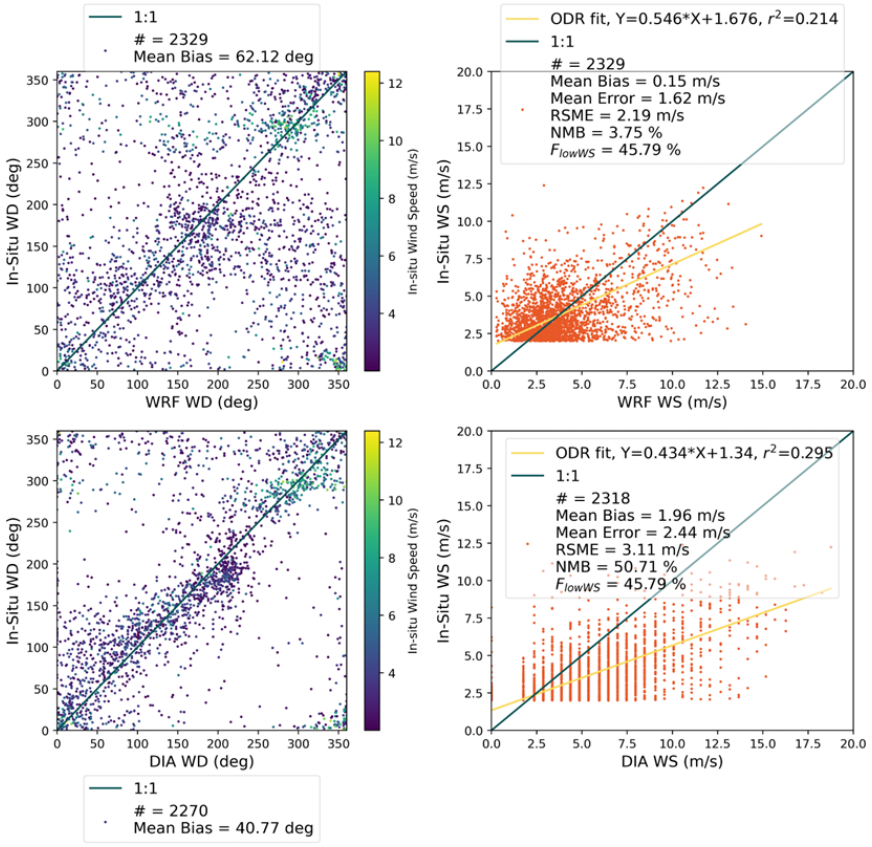

Figure C5. Hourly wind direction and wind speed comparison between in situ observations and WRF and DIA for January to June 2022, after removing low wind speed (<2 m/s). Wind directions are colored by wind speed. FlowWS is the fraction of WS smaller than 2 m/s.

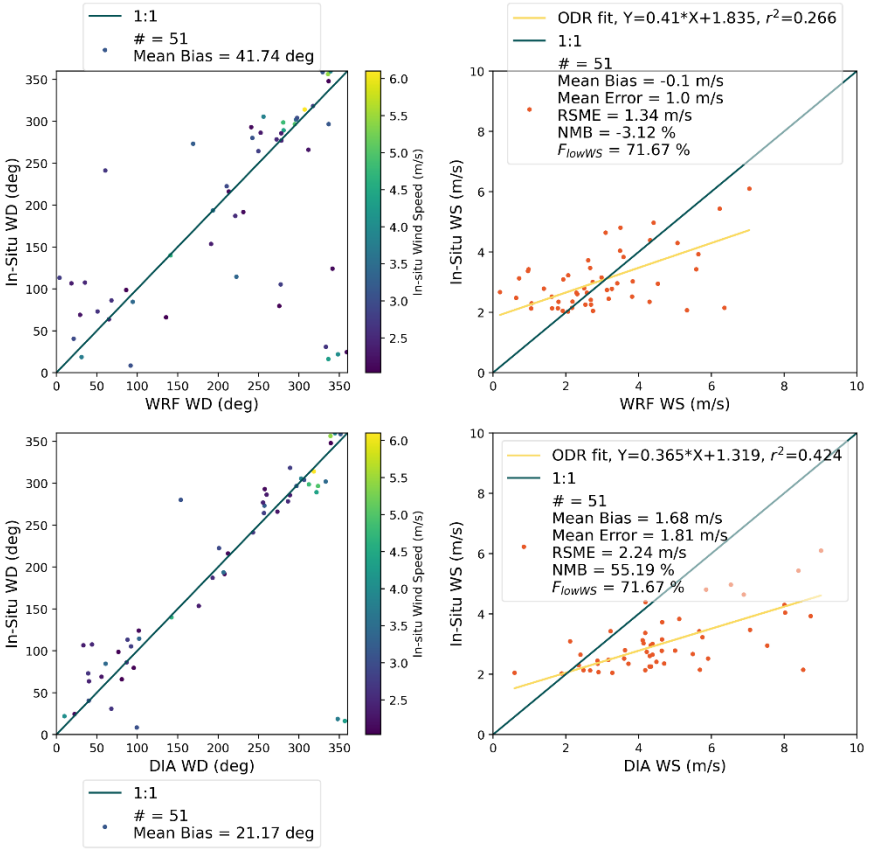

Figure C6. Daily wind direction and wind speed comparison between in situ observations and WRF and DIA for January to June 2022 after removing low wind speed (<2 m/s). Wind directions are colored by wind speed. FlowWS is the fraction of WS smaller than 2 m/s.

C.3. Model Validation Using C8-C10 n-Alkanes Measured in Broomfield

As useful tracers for drilling operations using Neoflo mud, C_8–C_{10} n-alkanes have low background concentrations and well-defined sources (Ku et al., 2024); therefore, we first quantify the emission rates of these three tracers during drilling operations to assess AERMOD performance. The performance of weekly AERMOD simulations using inversion-based emission rates is evaluated by comparing the predicted and observed concentrations of C_8–C_{10} n-alkanes (Figure C7). The regression slope, correlation (r^2), and overall mean bias between predicted and observed concentrations are 0.99, 0.88, and −0.19 µg/m^3, respectively. The MLR method, combined with AERMOD simulations and in situ observations, predicts C_8–C_{10} n-alkane concentrations with low mean bias and good correlation.

Our evaluation reveals that the MLR-inversion method appropriately assigns C_8–C_{10} n-alkane emissions to well pad locations with active drilling operations and does not assign significant C_8–C_{10} alkane emissions to other well pad locations (see Figure C8).

This test gives us added confidence in using the MLR inversion method to obtain emission rates of other VOCs during UOGD operations. Detailed results and additional model evaluation for all UOGD operations and selected VOCs are provided in Figure C9.

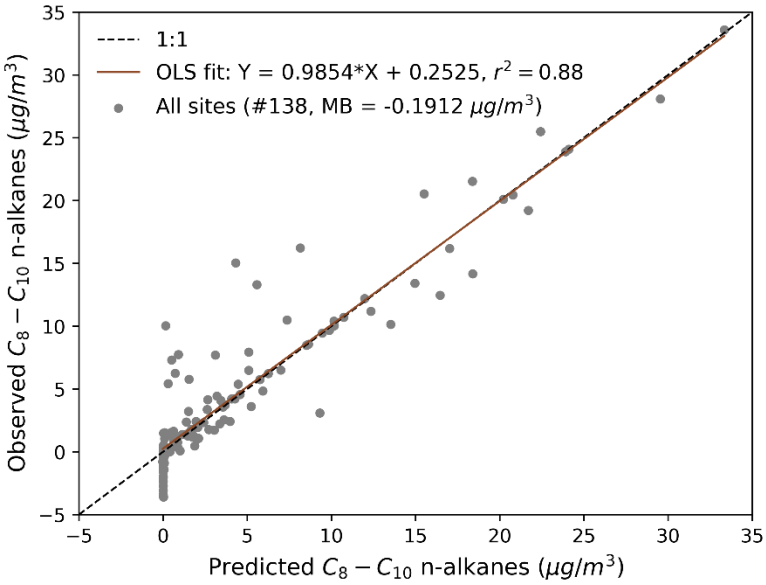

Figure C7. Observed vs. predicted C8–C10 n-alkane concentrations during drilling operations. Observed concentrations are from weekly canister samples, while predicted concentrations are the AERMOD simulation results using MLR-constrained emission rates**.** Both concentrations are the results after subtracting regression constants (i.e., regional background). The black line shows the 1:1 line, and the brown line shows the ordinary least square regression result for all data, with corresponding regression parameters shown in the legend. In the legend, "#" represents the number of weekly concentrations, and MB is the mean bias of all predicted concentrations.

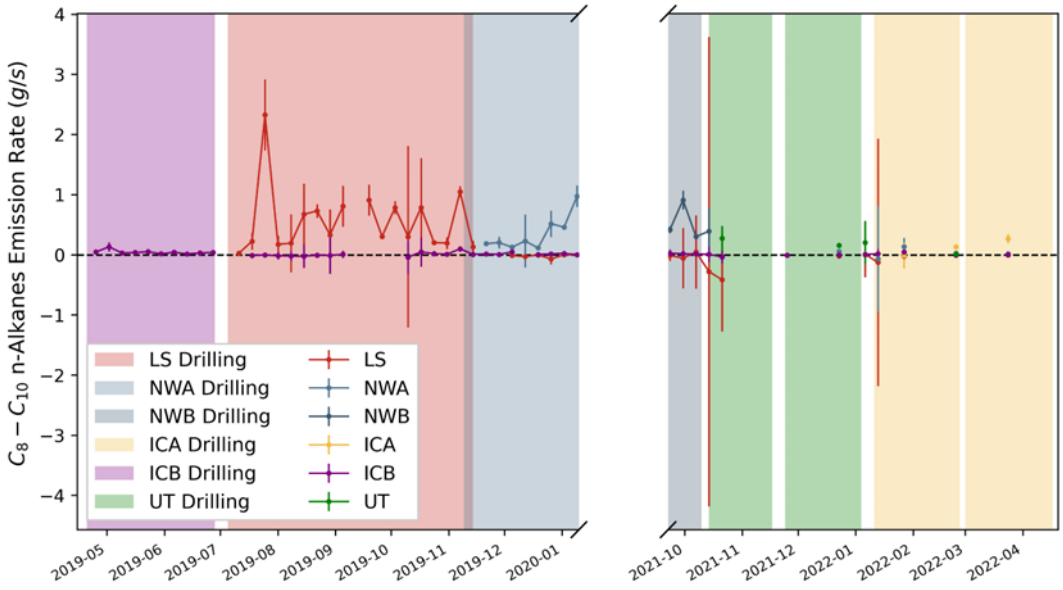

Figure C8. Constrained emission rates of C_8-C_{10} n-alkanes for periods with drilling operations. The error bar represents the uncertainty of the corresponding emission rate. Solid lines and colored areas represent the emission rates and drilling periods of different O&G well pads, respectively.

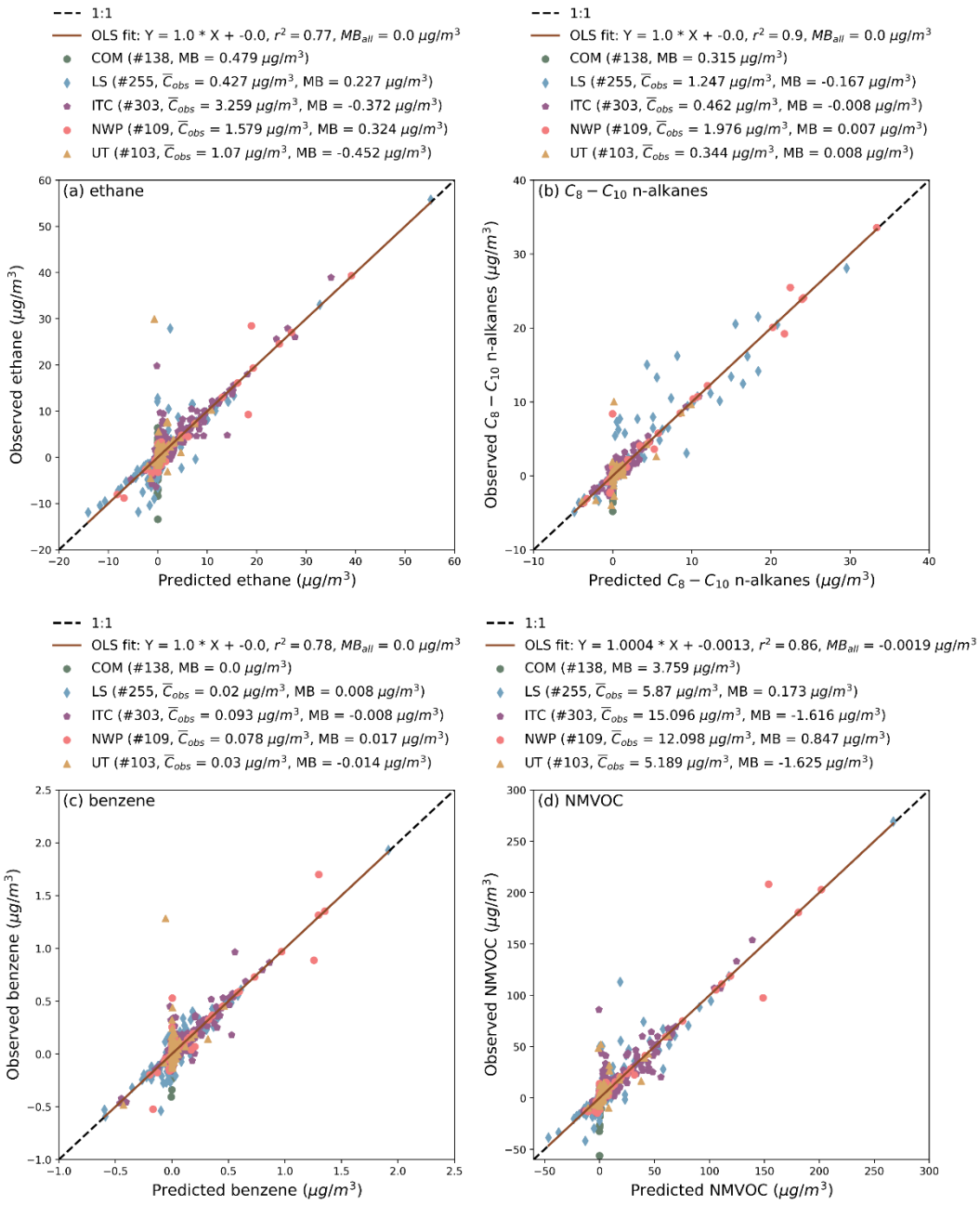

Figure C9. Observed VOC concentrations vs. predicted VOC concentrations for all operations. The observed concentrations are weekly canister sample concentrations. The predicted concentrations are the AERMOD simulation results with the MLR constrained emission rates. Both concentrations are the results after subtracting regression constants. Panels (a)–(d) show observed and predicted ethane, C_8–C_{10}, benzene, and NMVOC (non-methane VOC), respectively. Black lines show the 1:1 line. Brown lines show ordinary least square regression results for all data. The corresponding regression parameters and evaluation statistics are shown in the legends. Adjacent monitoring sites are labeled as a single category. For example, in the plots, ITC01, ITC02, and ITC03 are all labeled as ITC. Same with LS and UT. In the legend, "#" represents the number of weekly concentrations; $\overline{\boldsymbol{C}}_{\boldsymbol{obs}}$ is the mean observed concentrations; MB is the mean bias of predicted concentration from each category; and MB_{all} is the mean bias of all predicted concentrations.

C.4. Emission Rates from the Inversion Method (Zhang et al. 2025), Hecobian et al. 2019), and EPA Emission Tool (US EPA 2020)

Table C1. Median Emission Rates and Uncertainties of Select VOCs for Drilling Operations: This Study (Weekly Samples) vs. EPA Emission Tool vs. Hecobian et al. (2019**)**

VOC	This Study Drilling Gibson Mud Median (Uncertainty) Emission Rates (g/s)	This Study Drilling Neoflo Mud Median (Uncertainty) Emission Rates (g/s)	EPA Emission Tool Oil-based or Synthetic-based Drilling Mud Degassing Emission Rate (g/s)	Hecobian et al. Drilling Median Emission Rate (g/s) – Piceance Basin
Ethane	0.11419 (± 0.08418)	0.22568 (± 0.45397)	NA	0.13
Propane	0.08477 (± 0.08401)	0.27353 (± 0.29604)	NA	0.12
C_8-C_{10} n-alkanes	0.03908 (± 0.01774)	0.303 (± 0.14086)	NA	0.007
Benzene	0.00404 (± 0.00457)	0.00986 (± 0.0102)	NA	0.004
Toluene	0.01201 (± 0.01162)	0.02973 (± 0.03768)	NA	0.088
Ethylbenzene	0.00204 (± 0.00207)	0.00357 (± 0.00714)	NA	0.0009
Xylenes	0.01448 (± 0.01064)	0.03304 (± 0.02544)	NA	0.004
Ethyne	0.00011 (± 0.00138)	-0.00101 (± 0.00709)	NA	NA
NMVOC	0.48144 (± 0.15535)	1.9447 (± 0.8688)	0.36	0.43

"NA" denotes no available value.

Table C2. Median Emission Rates and Uncertainties of Select VOCs for Hydraulic Fracturing Operations: This Study (Weekly Samples) vs. EPA Emission Tool vs. Hecobian et al. (2019)

VOC	This Study Fracking Median (Uncertainty) Emission Rates (g/s)	EPA Emission Tool Fracking 700 hp Engine Emission Rate (g/s)	EPA Emission Tool Fracking 1500 hp Engine Emission Rate (g/s)	Hecobian et al. (2019) Fracking Median Emission Rate (g/s) – DJ Basin
Ethane	−0.05019 (± 0.15957)	NA	NA	0.0026
Propane	0.00117 (± 0.11467)	NA	NA	0.0005
C_8-C_{10} n-alkanes	−0.00784 (± 0.02886)	NA	NA	0.0105
Benzene	−0.0002 (± 0.00565)	0.002	0.0042	0.0022
Toluene	−0.00214 (± 0.00988)	0.0014	0.003	0.0056

VOC	This Study Fracking Median (Uncertainty) Emission Rates (g/s)	EPA Emission Tool Fracking 700 hp Engine Emission Rate (g/s)	EPA Emission Tool Fracking 1500 hp Engine Emission Rate (g/s)	Hecobian et al. (2019) Fracking Median Emission Rate (g/s) – DJ Basin
Ethylbenzene	−0.00038 (± 0.00258)	0.0002	0.0004	0.0008
Xylenes	−0.00201 (± 0.00723)	0.0005	0.0011	0.0056
Ethyne	0.02129 (± 0.01351)	NA	NA	NA
NMVOC	−0.01659 (± 0.28579)	0.04	0.08	0.08

"NA" denotes no available value.

Table C3. Median Emission Rates and Uncertainties of Select VOCs for Flowback Operations: This Study (Weekly Samples) vs. EPA Emission Tool vs. Hecobian et al. (2019)

VOC	This Study Flowback Median (Uncertainty) Emission Rates (g/s)	EPA Emission Tool Flowback Green-Completion Emission Rate (g/s)	Hecobian et al. (2019) Flowback Median Emission Rate (g/s) – DJ Basin
Ethane	0.01756 (± 0.11715)	0	1.1
Propane	0.04053 (± 0.1101)	0	0.75
C_8-C_{10} n-alkanes	0.01097 (± 0.01215)	0	0.342
Benzene	0.00126 (± 0.0053)	0	0.069
Toluene	−5e-05 (± 0.02283)	0	0.21
Ethylbenzene	0.00013 (± 0.00279)	0	0.019
Xylenes	0.00203 (± 0.00546)	0	0.274
Ethyne	0.00035 (± 0.00426)	0	NA
NMVOC	0.09456 (± 0.24001)	0	6.33

"NA" denotes no available value.

Table C4. Median Emission Rates and Uncertainties of Select VOCs for Production Operations: This Study (Weekly Samples) vs. EPA Emission Tool vs. Hecobian et al. (2019)

VOC	This Study Production Median (Uncertainty) Emission Rates (g/s)	EPA Emission Tool Flowback Green-Completion Emission Rate (g/s/well)	Hecobian et al. (2019) Production Median Emission Rate (g/s) – DJ Basin
Ethane	0.02004 (± 0.1466)	NA	0.1
Propane	0.02803 (± 0.11653)	NA	0.088
C_8-C_{10} n-alkanes	0.00015 (± 0.0135)	NA	0.0021
Benzene	0.00013 (± 0.0085)	0.0015	0.0013
Toluene	−0.00058 (± 0.02157)	0.0001	0.0011
Ethylbenzene	−0.00027 (± 0.00475)	0.000007	0.0002
Xylenes	−0.00081 (± 0.01683)	0.0025	0.0016
Ethyne	9e-05 (± 0.01014)	NA	NA
NMVOC	0.0857 (± 0.2941)	0.055	0.33

"NA" denotes no available value.

C.5. Simulations with Mean Inverted Emission Rates

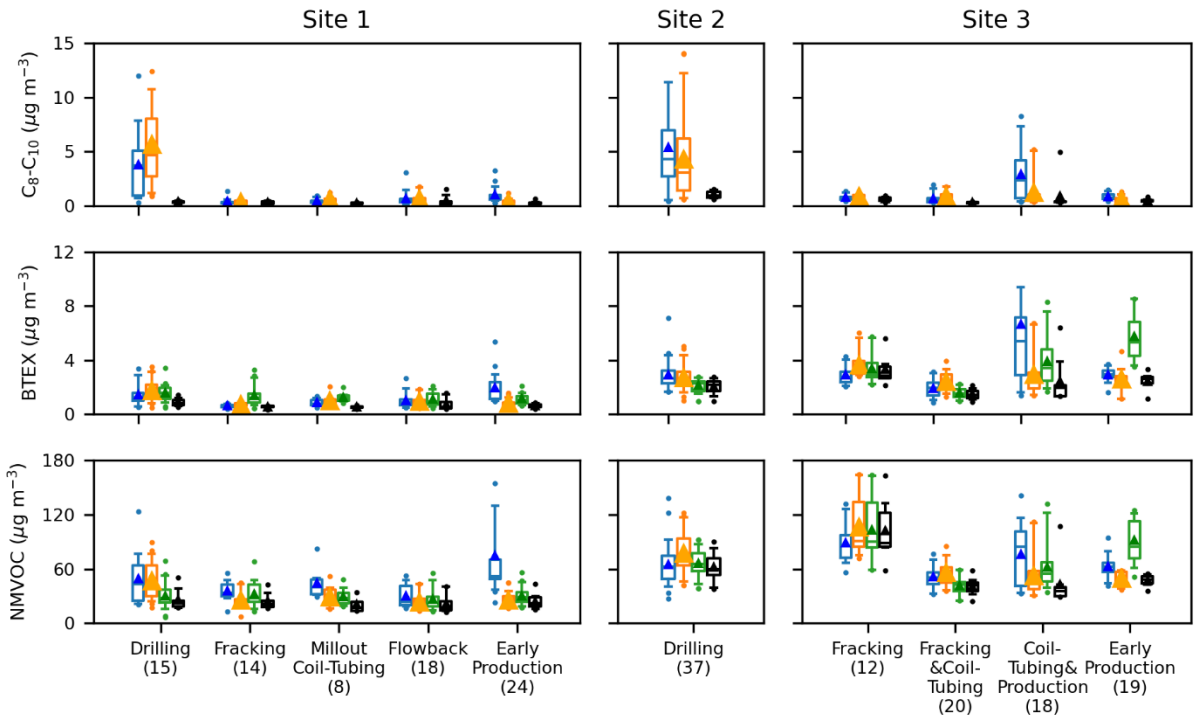

Figure C10. Boxplots of observed and simulated weekly integrated VOC concentrations. The simulations were conducted with mean inverted emission rates.

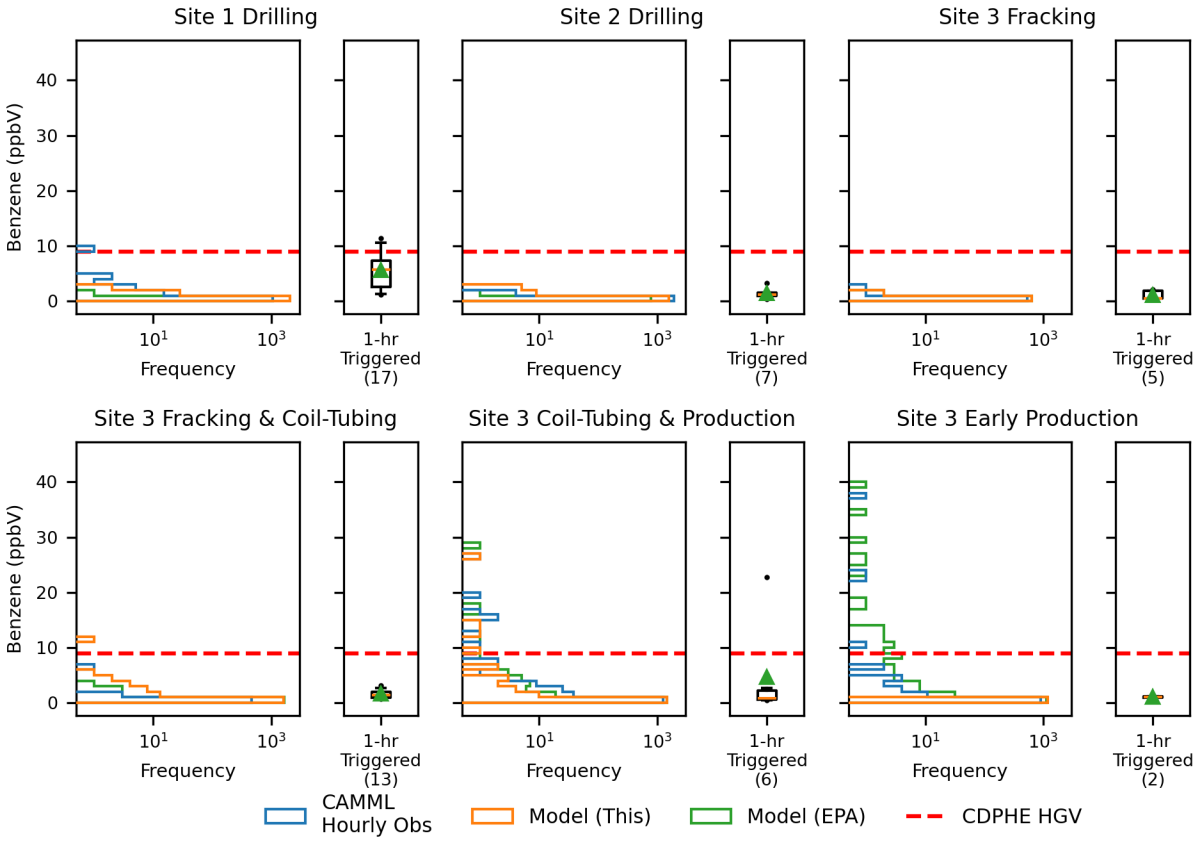

Figure C11. Histograms of simulated and observed hourly benzene concentrations and 1-hour extrapolated benzene concentrations from triggered canisters. The simulations were conducted with mean inverted emission rates.

C.6. AERMOD Simulation Errors vs. Measurement Uncertainties

Table C5. Mean Percent Errors of AERMOD Simulations and Measurement Uncertainties for 50 VOCs

VOC	AERMOD Simulation Mean Percent Error (%)	Measurement Uncertainty (%)
ethane	89.96	6.55
propane	81.03	5.46
i-butane	89.81	5.35
n-butane	161.18	5.51
i-pentane	95.62	5.34
n-pentane	101.51	5.64
n-hexane	128.74	5.84
n-heptane	89.58	6.25
n-octane	107	5.67
n-nonane	119.36	6.02
n-decane	198.12	6.54
cyclopentane	455.98	5.36
cyclohexane	101.94	5.52
methylcyclohexane	88.86	6.27
2,3,4 tmp	95.47	5.63
2,2,4-trimethylpentane	96.17	16.9
2,3-dmp	147.05	5.48
2,4 dimethylpentane	119.61	6.82
2-methylhexane	262.46	5.67
3-methylhexane	236.63	5.85
2-methylheptane	154.14	5.68
3-methylheptane	127.06	5.7
ethene	2289.48	5.54
propene	141.38	5.7
t-2-butene	104.55	5.4
1-butene	105.59	5.35
c-2-butene	112.01	5.32
t-2-pentene	157.65	5.74
1-pentene	91.07	6.71
cis-2-pentene	93.98	7.68
benzene	187.35	5.77
toluene	105.29	5.74
ethylbenzene	118.11	6.04
m+p-xylene	102.36	6.58
o-xylene	115.1	6.19
styrene	122.06	23.51
i-propylbenzene	86.25	22.23
n-propylbenzene	115.98	16.71
3-ethyltoluene	176.87	18.45
4-ethyltoluene	100.82	23.53
2-ethyltoluene	84.46	19.98
1,3,5-trimethylbenzene	133.95	13.93
1,2,4-trimethylbenzene	129.95	18.68
1,2,3-trimethylbenzene	159.99	20.66
1,3-diethylbenzene	116.03	15.42
1,4-diethylbenzene	103.71	18.72
ethyne	116.03	6.26
isoprene	93.71	6.54
c2cl4	100.18	10.6
c2hcl3	131.54	12.21

Note: Mean percent error of AERMOD simulation is the percentage form of mean relative change calculated from the absolute change between the AERMOD simulated concentrations and measured concentrations, and divided by the measured concentrations for all UOGD operations.

C.6. References

Hecobian, A., Clements, A. L., Shonkwiler, K. B., Zhou, Y., MacDonald, L. P., Hilliard, N., Wells, B. L., Bibeau, B., Ham, J. M., & Pierce, J. R. (2019). Air toxics and other volatile organic compound emissions from unconventional oil and gas development. Environmental Science & Technology Letters, 6(12), 720-726.

Ku, I.-T., Zhou, Y., Hecobian, A., Benedict, K., Buck, B., Lachenmayer, E., Terry, B., Frazier, M., Zhang, J., & Pan, D. (2024). Air quality impacts from the development of unconventional oil and gas well pads: Air toxics and other volatile organic compounds. Atmospheric Environment, 317, 120187.

Perry, S. G., Cimorelli, A. J., Paine, R. J., Brode, R. W., Weil, J. C., Venkatram, A., Wilson, R. B., Lee, R. F., & Peters, W. D. (2005). AERMOD: A dispersion model for industrial source applications. Part II: Model performance against 17 field study databases. Journal of Applied Meteorology, 44(5), 694-708.

Stull, R. B. (1988). Mean boundary layer characteristics. In: An Introduction to Boundary Layer Meteorology (pp. 1-27). Springer.

US EPA. (2020). 2020 EPA Nonpoint Oil and Gas Emissions Estimation Tool.

Zhang, W., Pan, D., Ku, I.-T., Pierce, J., & Collett, J. J. (2025). Using ambient concentration measurements to quantify volatile organic compound emissions from unconventional oil and gas operations. Environmental Science & Technology Letters, 16 December 2025.